Available online at www.sciencedirect.com
SCIENCE DIRECT®
Journal of Computational Physics 197 (2004) 99–115
JOURNAL OF COMPUTATIONAL PHYSICS
www.elsevier.com/locate/jcp

An algebraic method to develop well-posed PML models Absorbing layers, perfectly matched layers, linearized Euler equations

Adib N. Rahmouni

Department of Mathematics, LAGA, Université Paris, Paris 13, France

Received 22 March 2001; received in revised form 23 October 2003; accepted 18 November 2003
Available online 17 January 2004

Abstract

In 1994, Bérenger [Journal of Computational Physics 114 (1994) 185] proposed a new layer method: *perfectly matched layer*, PML, for electromagnetism. This new method is based on the truncation of the computational domain by a layer which absorbs waves regardless of their frequency and angle of incidence. Unfortunately, the technique proposed by Bérenger (loc. cit.) leads to a system which has lost the most important properties of the original one: strong hyperbolicity and symmetry. We present in this paper an algebraic technique leading to well-known PML model [IEEE Transactions on Antennas and Propagation 44 (1996) 1630] for the linearized Euler equations, strongly well-posed, preserving the advantages of the initial method, and retaining symmetry. The technique proposed in this paper can be extended to various hyperbolic problems.

1. Introduction

The numerical study of wave propagation problems in unbounded domains requires to create a finite computational region and thus the introduction of an artificial boundary. Several methods have been proposed to reduce the problem to a bounded domain. Some of them have an empirical origin: *the absorbing layers methods*, others are based on a theoretical approach: *the integral equations and the absorbing boundary conditions*.

The strategy of absorbing boundary conditions consists in imposing on the artificial boundary a differential operator, thereby local, to create a finite computational region. These methods have been widely studied by mathematicians [10] for different kind of problems (see [11,28] in fluid dynamics); one of the disadvantages of these methods remains the corner problem for which there is no general theory and their implementation is quite intricate.

E-mail address: rahmouni@math.univ-paris13.fr (A.N. Rahmouni).

0021-9991/$ - see front matter © 2003 Elsevier Inc. All rights reserved.
doi:10.1016/j.jcp.2003.11.019

The integral equation methods consist in reducing the infinite domain into a bounded one, replacing the outer problem by boundary elements formulation (on the artificial boundary) based on an integral representation of the exact solution in the exterior. This method gives rise to an exact and global operator which leads to large full matrices.

The layer or sponge methods consist of surrounding the domain of interest by a layer. This layer should be designed such that it produces as low reflection as possible and the waves are absorbed in the layer. Furthermore to save computation, it should be made thin.

In practice, defining the layer can be very involved as it is very much depending on the frequency of the incoming signal. This explains why layer methods have not been very much used. More evolved models have been proposed (coupling layers and absorbing boundary conditions) [15], but the increase of complexity lessens the interest of these methods.

Bérenger's work [4] has renewed the interest in these layer methods; the Bérenger perfectly matched layer, PML, has many attractive features: it absorbs waves of any wavelength and any frequency without spurious reflection; moreover, the corner problem is easily solved by a wise choice of the layer parameters. Finally, it is very easy to integrate into an existing code.

Unfortunately, as applied to the Maxwell system, the original method leads to a system which has lost the most important properties of the Maxwell system: strong hyperbolicity and symmetry.

We propose in the last part an algebraic technique leading to a new PML model which is strongly well-posed and preserves the symmetry.

2. The classical layer technique

The methods of layers consist in surrounding the domain of interest (where we want to compute the solution) with an absorbing layer. This layer must be such that the transmission of a wave propagating from the domain of interest into the layer is reflectionless.

These layer techniques are often inspired by well-known physical models (soundproof rooms of acoustics laboratories). As an example, we first present some models for the wave equation in two dimensions of space. These examples, although simple, highlight the power and the limitations of the classical approach. We summarize here some of the results by Israeli and Orszag [15].

We consider the wave equation in two dimensions

$$\frac{\partial^2 u}{\partial t^2} - \Delta u = 0. \tag{1}$$

A simple model has been written in [15] by adding a friction term

$$\frac{\partial^2 u}{\partial t^2} + \sigma(x)\frac{\partial u}{\partial t} - \Delta u = 0. \tag{2}$$

In such medium, for $\sigma > 0$, the energy decreases: it is a lossy medium.

More precisely, we consider the case of a propagation in the half space $x < 0$, and we construct the layer of width δ on the right of the domain. The problem is written as

$$\begin{cases} \frac{\partial^2 u}{\partial t^2} + \sigma(x)\frac{\partial u}{\partial t} - \Delta u = 0, & (x,y) \in]-\infty,\delta[\times\mathbb{R} \\ u_{t=0} = u_0, \quad \left(\frac{\partial u}{\partial t}\right)_{t=0} = u_1, \\ u(\delta,y,t) = 0, \end{cases} \tag{3}$$

where $\sigma(x)$ vanishes for $x < 0$ and the initial data are supported in $\mathbb{R}_- \times \mathbb{R}$. In the domain of interest (here the half space $x < 0$) we recover the classical wave equation. The model is valid if the layer does not generate reflections for a wave crossing the interface between the domain of interest and the layer. Therefore, the choice of the dumping factor σ is paramount. Moreover, the decay of the wave in the layer must be sufficiently significant so that the Dirichlet [1] condition imposed on the exterior boundary of the layer does not generate important reflections (see also [7]).

The plane wave analysis gives a more precise idea of the good choice of the damping factor. So let $u_i = \mathrm{e}^{\mathrm{i}(k_x x + k_y y - \omega t)}, k_x/\omega > 0$ be an incident plane wave in $]-\infty, 0[\times\mathbb{R}$, with the dispersion relation $k_x^2 + k_y^2 = \omega^2$. The solution of (3) is given by

$$\begin{cases} u = \mathrm{e}^{\mathrm{i}(k_x x + k_y y - \omega t)} + R\mathrm{e}^{\mathrm{i}(-k_x x + k_y y - \omega t)} & \text{in }]-\infty, 0[\times\mathbb{R}, \\ u = T_1 \mathrm{e}^{\mathrm{i}(k_x^\sigma x + k_y y - \omega t)} + T_2 \mathrm{e}^{\mathrm{i}(-k_x^\sigma x + k_y y - \omega t)} & \text{in }]0, \delta[\times\mathbb{R}, \\ k_x^2 + k_y^2 = \omega^2, \quad (k_x^\sigma)^2 = k_x^2 + \mathrm{i}\omega\sigma, \\ \frac{k_x}{\omega} > 0, \quad k_x^\sigma \in \mathbb{C}, \quad \frac{\Re k_x^\sigma}{\omega} > 0 \end{cases} \tag{4}$$

with

$$\begin{cases} R = \frac{R_0 + R_\delta}{1 + R_0 R_\delta}, \quad R_0 = \frac{k_x - k_x^\sigma}{k_x + k_x^\sigma}, \quad T_1 = \frac{1+R}{1+R_\delta}, \\ T_2 = R_\delta T_1, \quad R_\delta = -\mathrm{e}^{2\mathrm{i}k_x^\sigma \delta}. \end{cases} \tag{5}$$

The goal now was to choose the optimal damping factor σ to make the module of R as small as possible independently of the frequencies and the angle of incidence. First, let us expand the reflection coefficient in the form

$$R = R_0 + R_\delta (R_0^2 - 1) \sum_{n \geqslant 0} (R_\delta R_0)^n, \tag{6}$$

R_0 is the part of the reflection coefficient at the entrance of the layer (due to the change of medium) whereas R_δ is the part due the Dirichlet condition imposed on the exterior boundary of the layer.

If σ is too large then R_0 is large too. In fact the incident wave sees a brutal change of the medium's characteristics (σ jump from zero to a large value) leading to spurious reflections.

In the same manner, when σ is too small, R_δ becomes significant: the wave arriving on the exterior boundary is not sufficiently absorbed, the spurious reflections are then due to the Dirichlet condition imposed on this boundary.

3. A well-posed PML model

Although they are easier to implement than the absorbing boundary conditions, the classical layer methods have not often been used because of the inconveniences seen before.

In [4] Bérenger proposed a new layer method, *perfectly matched layer*, for electromagnetism. The original Bérenger technique has been extended to various hyperbolic problems [2,5,8,14,17–22].

In [14] the author presents the PML model obtained by the Bérenger approach for the linearized Euler equations; as shown in [14] this model presents attractive properties that the theoretical reflection coefficient at an interface between the domain of interest and the PML layer is zero for all frequencies and angles of incidence. Moreover, the wave is exponentially decaying in the layer which allow to impose a Dirichlet condition on the external boundary. However, the time-domain model obtained by the Bérenger approach presents some inconveniences; unlike the original system the new one is only weakly hyperbolic and we have lost the symmetry [2].

[1] To keep the model as simple as possible.

Various PML models have been proposed to circumvent the problems mentioned above; in [2,12], the authors (following the approach developed for electromagnetism in [1]) modify the Euler equations by introducing low-order terms, obtaining by construction a well-posed model. We propose an algebraic technique leading to a PML model, strongly well-posed preserving the advantages of the initial method and retaining symmetry. Moreover, this model uses primitive variables unlike the Bérenger model. In fact (for the choice corresponding to N diagonal, see below) the model obtained is identical to the model obtained for frequency domain FEM in [25] and also for FDTD by Gedney in [9] (also Chapter 5 in [26]). Our model is similar to the model obtained in [12], a detailed analysis can be found in [1]. However, the approach used is radically different; unlike the model proposed in [12], which is based on a modification of the Euler equations, ours is based on the Bérenger technique, thus this method can be generalized to other hyperbolic problems [21].

We first define a PML medium.

Definition 3.1. For a first order hyperbolic system, $\mathscr{L}u = 0$, we have the following definition:

- A layer model for the problem $\mathscr{L}u = 0$ in $]-\infty, 0] \times \mathbb{R}$ is such that

$$\begin{cases} \mathscr{L}_\sigma u = 0 & \text{in }]-\infty, \delta] \times \mathbb{R}, \\ \mathscr{L}_\sigma u = \mathscr{L}u & \text{in } \mathbb{R}_- \times \mathbb{R}. \end{cases}$$

- A layer model is a PML model if
  - Reflectionless transmission between the domain of interest and the layer regardless frequency and angle of incidence.
  - Exponential decay of the solution in the layer.

We shall adopt the above definition in all the sections below.

3.1. The quiescent free-stream

We start from the time-harmonic unsplit model

$$\mathrm{i}\omega\phi + \left(S_x A \frac{\partial \phi}{\partial x} + S_y B \frac{\partial \phi}{\partial y} \right) = 0 \tag{7}$$

with

$$S_x = \frac{\mathrm{i}\omega}{\mathrm{i}\omega + \sigma_1(x)} \quad \text{and} \quad S_y = \frac{\mathrm{i}\omega}{\mathrm{i}\omega + \sigma_2(y)}.$$

This model preserves all the properties of the Bérenger model: reflectionless interface between two PML medium provided that σ_1 and σ_2 are well chosen, exponential decrease of the solution in the layer (see [6]).

In order to obtain a well-posed time-domain PML model, we rewrite the spatial operator $S_x A \partial_x + S_y B \partial_y$ using the original operator.

Lemma 3.1. *There exist two invertible operators, M and N, such that*

$$S_x A \partial_x + S_y B \partial_y = M(A\partial_x + B\partial_y)N \tag{8}$$

which furthermore have the properties

$$A\partial_x N + B\partial_y N = 0 \quad \textit{and} \lim_{\sigma_1, \sigma_2 \to 0} N = I. \tag{9}$$

Proof. First, we seek all invertible operators M and N such that

$$\begin{aligned} MAN - S_x A &= 0, \\ MBN - S_y B &= 0. \end{aligned} \tag{10}$$

Since M and N are invertible, we can rewrite (10) as follows:

$$\begin{aligned} AN - S_x M^{-1} A &= 0, \\ BN - S_y M^{-1} B &= 0. \end{aligned} \tag{11}$$

Since $\ker(A) = \mathrm{vect}(e_2)$, this implies that Ne_2 belongs to $\ker(A)$, or $Ne_2 = \lambda e_2$. In the same way, since $\ker(B) = \mathrm{vect}(e_1)$ we must have $Ne_1 = \mu e_1$; where (e_i) denotes the canonical basis of $\mathbb{R}^3$.

We deduce the general form of N:

$$N = \begin{pmatrix} \mu & 0 & n_{13} \\ 0 & \lambda & n_{23} \\ 0 & 0 & n_{33} \end{pmatrix}.$$

We can note that if (M,N) is a solution of (10), then $({}^tN, {}^tM)$ is a solution of (10), hence

$$M = \begin{pmatrix} m_{11} & 0 & 0 \\ 0 & m_{22} & 0 \\ m_{31} & m_{32} & m_{33} \end{pmatrix}$$

thus, using $Ne_2 = \lambda e_2$, we have $\mu Me_3 = S_x e_3$, and in the same manner $Ne_1 = \mu e_1$ gives $\mu Me_3 = S_x e_3$.

Finally, we find the general form of M and N solution of (10)

$$N = \begin{pmatrix} S_x S_y^{-1} \lambda & 0 & n_{13} \\ 0 & \lambda & n_{23} \\ 0 & 0 & n_{33} \end{pmatrix} \quad \text{and} \quad M = \begin{pmatrix} S_x n_{33}^{-1} & 0 & 0 \\ 0 & S_y n_{33}^{-1} & 0 \\ -\lambda^{-1} n_{13} S_y n_{33}^{-1} & -\lambda^{-1} n_{23} S_y n_{33}^{-1} & \lambda^{-1} S_y \end{pmatrix}. \tag{12}$$

For simplicity we choose here N to be diagonal

$$N = \begin{pmatrix} S_y^{-1} & 0 & 0 \\ 0 & S_x^{-1} & 0 \\ 0 & 0 & 1 \end{pmatrix} \quad \text{and} \quad M = \begin{pmatrix} S_x & 0 & 0 \\ 0 & S_y & 0 \\ 0 & 0 & S_x S_y \end{pmatrix}.$$

This choice implies that (9) is satisfied.

Using the previous lemma, (7) becomes

$$\mathrm{i}\omega\phi + M(A\partial_x + B\partial_y)(N\phi) = 0$$

and the change of unknown $\tilde{\phi} = N\phi$ gives

$$\mathrm{i}\omega M^{-1} N^{-1} \tilde{\phi} + (A\partial_x + B\partial_y)(\tilde{\phi}) = 0.$$

In order to establish the time-dependent model, we start by writing the operator $\mathrm{i}\omega M^{-1} N^{-1}$ in the form

$$\mathrm{i}\omega M^{-1} N^{-1} = \mathrm{i}\omega \begin{pmatrix} S_x^{-1} S_y & & \\ & S_x S_y^{-1} & \\ & & S_x^{-1} S_y^{-1} \end{pmatrix} = \mathrm{i}\omega I + C + RU_\omega \tag{13}$$

with

$$C = \begin{pmatrix} \sigma_x - \sigma_y & & \\ & \sigma_y - \sigma_x & \\ & & \sigma_x + \sigma_y \end{pmatrix}, \quad R = \begin{pmatrix} \sigma_y(\sigma_y - \sigma_x) & & \\ & \sigma_x(\sigma_x - \sigma_y) & \\ & & -\sigma_x\sigma_y \end{pmatrix} \quad \text{and}$$

$$U_\omega = \begin{pmatrix} (\mathrm{i}\omega + \sigma_y)^{-1} & & \\ & (\mathrm{i}\omega + \sigma_x)^{-1} & \\ & & (\mathrm{i}\omega)^{-1} \end{pmatrix}.$$

Finally, the time-harmonic model becomes

$$\mathrm{i}\omega\tilde{\phi} + C\tilde{\phi} + RU_\omega\tilde{\phi} + (A\partial_x + B\partial_y)(\tilde{\phi}) = 0. \qquad \square \tag{14}$$

Remark. The new unknown $\tilde{\phi}$ is equal to the original one, ϕ, in the domain of interest (i.e. when $\sigma_x = \sigma_y = 0$). Moreover, when transmitted to the PML the new unknown $\tilde{\phi}$ does not "see" a contrast between the two medium (due to $\lim_{\sigma_1,\sigma_2 \to 0} N = I$). Finally, this change of unknown can be interpreted as a complex change of basis ($S_x A = MAN$) in agreement with the interpretation given in [23] of the Bérenger layer.

By an inverse Fourier transform of (14), we obtain the time-domain model (where $K \overset{t}{*} \tilde{\phi}$ represents the convolution in time)

$$\partial_t\tilde{\phi} + C\tilde{\phi} + RK \overset{t}{*} \tilde{\phi} + (A\partial_x + B\partial_y)(\tilde{\phi}) = 0 \tag{15}$$

with

$$K = \begin{pmatrix} \mathrm{e}^{-\sigma_y t} & & \\ & \mathrm{e}^{-\sigma_x t} & \\ & & 1 \end{pmatrix}. \tag{16}$$

The system above is not local in time. Increasing the number of unknowns (this is a classical technique in the study of dispersive materials [26]), we localize it by introducing a new unknown, T, which is solution of an ordinary differential equation, it then becomes

$$\begin{cases} \partial_t\tilde{\phi} + C\tilde{\phi} + RT + (A\partial_x + B\partial_y)(\tilde{\phi}) = 0, \\ \partial_t T + DT - \tilde{\phi} = 0 \end{cases} \tag{17}$$

with

$$D = \begin{pmatrix} \sigma_y & & \\ & \sigma_x & \\ & & 0 \end{pmatrix} \tag{18}$$

or

$$\partial_t \Phi + (\mathscr{C} + \mathscr{A}_{\partial_x,\partial_y})\Phi = 0, \tag{19}$$

where we have set

$$\Phi = \begin{pmatrix} \tilde{\phi} \\ T \end{pmatrix}, \quad \mathscr{C} = \begin{pmatrix} C & R \\ -I & D \end{pmatrix} \quad \text{and} \quad \mathscr{A}_{\partial_x,\partial_y} = \begin{pmatrix} A\partial_x + B\partial_y & 0 \\ 0 & 0 \end{pmatrix}. \tag{20}$$

At this point we can note that this model is the model obtained in [9] (and in the frequency domain in [25]).

Remark. In [24] the authors introduce a novel method which is based on a more general form of the stretched coordinates and on a recursive convolution; they also describe the discrete version of this convolutional PML. It would be very interesting to study the models obtained by the technique presented above in the case of more general form of the stretched-coordinate.

We can now state and prove our first result.

Theorem 3.1. *The model given by* (19) *is a PML model for the linearized Euler equations. Moreover, the Cauchy problem associated to this model is strongly well-posed and the solution is as smooth as the data.*

Proof. The Cauchy problem is

$$\begin{cases} \partial_t \Phi + \mathscr{A}_{\partial_x,\partial_y}\Phi + \mathscr{C}\Phi = 0, \\ \Phi(t=0) = \Phi_0, \end{cases} \tag{21}$$

where $\mathscr{A}_{\partial_x,\partial_y}$ and $\mathscr{C}$ have been defined in (20). The principal symbol of (21) is given by

$$\begin{pmatrix} A\xi_x + B\xi_y & 0 \\ 0 & 0 \end{pmatrix}. \tag{22}$$

Since the principal symbol is symmetric, the system (21) is strongly hyperbolic and therefore well-posed [16]. □

Remark. In practice it is preferable to choose a damping factor σ_x which does not become rapidly significant (for example parabolic) otherwise the wave crossing the interface between the mediums sees an abrupt change of the medium's characteristics leading to spurious reflection, this result is also valid for all layer methods. However in the PML medium, thanks to the exponential decay of the wave, this is not restrictive.

3.2. A family of well-posed PML models

Let us come back to the general form of M and N; as seen before the choice of a diagonal form for N is only for "morally" considerations. Indeed, using the general form of M and N the previous lemma gives

$$\begin{cases} \partial_x n_{13} + \partial_y n_{23} = 0, \\ \partial_x n_{33} = \partial_y n_{33} = \partial_y \lambda = 0, \\ \partial_x (S_x S_y^{-1} \lambda) = 0 \end{cases} \tag{23}$$

which leads to

$$n_{33} = 1 \quad \text{and} \quad \lambda = S_x^{-1}.$$

To satisfy the first equations of (23) we can choose (for example)

$$n_{13} = \alpha(y)(\mathrm{i}\omega)^{-1} \quad \text{and} \quad n_{23} = \beta(x)(\mathrm{i}\omega)^{-1}, \tag{24}$$

where α and β are equal to zero in the domain of interest in order to satisfy the lemma of the previous section (we can choose $\alpha = \sigma_y$ and $\beta = \sigma_x$. Following the previous study we obtain various PML models; for example choosing $\alpha = 0$ gives

$$N = \begin{pmatrix} S_y^{-1} & 0 & 0 \\ 0 & S_x^{-1} & \beta(x)(\mathrm{i}\omega)^{-1} \\ 0 & 0 & 1 \end{pmatrix} \quad \text{and} \quad M = \begin{pmatrix} S_x & 0 & 0 \\ 0 & S_y & 0 \\ 0 & -\beta(x)(\mathrm{i}\omega)^{-1}S_xS_y & S_xS_y \end{pmatrix},$$

then the change of unknowns $\tilde{\phi} = N\phi$ gives

$$\mathrm{i}\omega M^{-1}N^{-1}\tilde{\phi} + (A\partial_x + B\partial_y)(\tilde{\phi}) = 0,$$

which leads to the time-harmonic model

$$\mathrm{i}\omega\phi + C_2\tilde{\phi} + R_1U_\omega\tilde{\phi} + R_2V_\omega\tilde{\phi} + (A\partial_x + B\partial_y)(\tilde{\phi}) = 0, \tag{25}$$

where U_ω is given in the previous section and

$$C_2 = \begin{pmatrix} \sigma_x - \sigma_y & 0 & 0 \\ 0 & \sigma_y - \sigma_x & -\beta(x) \\ 0 & \beta(x) & \sigma_x + \sigma_y \end{pmatrix}, \quad V_\omega = \begin{pmatrix} 0 & 0 & 0 \\ 0 & 0 & 0 \\ 0 & 0 & (\mathrm{i}\omega + \sigma_x)^{-1} \end{pmatrix}.$$

$$R_1 = \begin{pmatrix} \sigma_y(\sigma_y - \sigma_x) & 0 & 0 \\ 0 & \sigma_x(\sigma_x - \sigma_y) & 0 \\ 0 & \beta(x)(\sigma_y - \sigma_x) & \beta^2(x)\sigma_x^{-1}\sigma_y - \sigma_x\sigma_y \end{pmatrix}, \tag{26}$$

$$R_2 = \begin{pmatrix} 0 & 0 & 0 \\ 0 & 0 & -\beta(x)(\sigma_y - \sigma_x) \\ 0 & 0 & \beta^2(x)\sigma_x^{-1}(\sigma_y - \sigma_x) \end{pmatrix}.$$

Finally, this model is given by (using an inverse Fourier transform)

$$\partial_t\tilde{\phi} + C_2\tilde{\phi} + R_1K \overset{t}{*}\tilde{\phi} + R_2K_2 \overset{t}{*}\tilde{\phi} + (A\partial_x + B\partial_y)(\tilde{\phi}) = 0, \tag{27}$$

where K is defined in (16) and $K_2 = \mathrm{diag}[0, 0, \mathrm{e}^{-\sigma_x t}]$.

Increasing the system above in the same way gives

$$\partial_t\Phi + (\mathscr{C} + \mathscr{A}_{\partial_x,\partial_y})\Phi = 0, \tag{28}$$

where we have set

$$\Phi = \begin{pmatrix} \tilde{\phi} \\ T_1 \\ T_2 \end{pmatrix}, \quad \mathscr{C} = \begin{pmatrix} C_2 & R_1 & R_2 \\ -I & D & 0 \\ -I & 0 & D_2 \end{pmatrix}, \quad \mathscr{A}_{\partial_x,\partial_y} = \begin{pmatrix} A\partial_x + B\partial_y & 0 & 0 \\ 0 & 0 & 0 \\ 0 & 0 & 0 \end{pmatrix}. \tag{29}$$

We can now state and prove that this model is again a well-posed PML model

Theorem 3.2. *The model given by* (28) *is a PML model for the linearized Euler equations. Moreover, the Cauchy problem associated to this model is strongly well-posed and the solution is as smooth as the data.*

Proof. Consider the Cauchy problem associated to this model

$$\begin{cases} \partial_t\Phi + \mathscr{A}_{\partial_x,\partial_y}\Phi + \mathscr{C}\Phi = 0, \\ \Phi_{t=0} = \Phi_0, \end{cases} \tag{30}$$

where $\mathscr{A}_{\partial_x,\partial_y}$ and $\mathscr{C}$ have been defined in (29). The principal symbol of (30) is given by

$$\begin{pmatrix} A\xi_x + B\xi_y & 0 & 0 \\ 0 & 0 & 0 \\ 0 & 0 & 0 \end{pmatrix} \tag{31}$$

The well-posedness is obtained exactly as in (21).

To establish now the PML properties of this model (according to the definition (3.1)). Following the analysis in [1], we shall consider the propagation of a plane wave in the two-dimensional case and for a half space (the general case can be analyzed using separation of variables); we consider a PML of thickness δ $(0 < x < \delta)$.

Let

$$\phi^- = \phi_0^- \mathrm{e}^{-\mathrm{i}(k_x x + k_y y - \omega t)} k_x^2 + k_y^2 = \omega^2$$

be an incident plane wave traveling from the domain of interest, $\Omega^- = \mathbb{R}^2_{\{x<0\}}$, where it satisfies the classical Euler equations to a PML medium $\Omega^+ = \mathbb{R}^2_{\{x>0\}}$ governed by the previous model. We shall seek ϕ in Ω^+ in the form

$$\phi^+ = \begin{pmatrix} u^+(x) \\ v^+(x) \\ p^+(x) \\ T_2^+(x) \\ T_3^+(x) \end{pmatrix} \cdot \mathrm{e}^{-\mathrm{i}(k_y y - \omega t)},$$

where we have set $(T_1)_2^+ = T_2^+$ and $(T_1)_2^+ = T_3^+$.

We can see that in the PML medium, Ω^+, u^+, v^+ and p^+ satisfy

$$\begin{cases} u^+ = (\mathrm{i}\omega + \sigma_x)^{-1}\partial_x p^+, \\ v^+ = -\frac{\mathrm{i}k_y(\mathrm{i}\omega+\sigma_x)}{(\mathrm{i}\omega)^2} p^+ + \frac{\beta(x)}{\mathrm{i}\omega} p^+, \\ \partial_x u^+ = (\mathrm{i}\omega + \sigma_x)p^+ - \left(\frac{k_y}{\omega}\right)^2 (\mathrm{i}\omega + \sigma_x)p^+. \end{cases} \tag{32}$$

Combining these equations yields the second order ordinary differential equation for $p^+(x)$

$$d_x((\mathrm{i}\omega + \sigma_x)^{-1} d_x p^+) - \left(\frac{k_x^2}{\omega^2}\right)(\mathrm{i}\omega + \sigma_x)p^+ = 0 \tag{33}$$

which has the general solution

$$p^+(x) = \kappa_1 \exp\left(\frac{k_x}{\omega}\int_0^x (\mathrm{i}\omega + \sigma_x(\xi))\,\mathrm{d}\xi\right) + \kappa_2 \exp\left(-\frac{k_x}{\omega}\int_0^x (\mathrm{i}\omega + \sigma_x(\xi))\,\mathrm{d}\xi\right). \tag{34}$$

Therefore, we deduce the expressions for the other components

$$\begin{cases} u^+(x) = \frac{k_x}{\omega}\left[\kappa_1 \exp\left(\frac{k_x}{\omega}\int_0^x (\mathrm{i}\omega + \sigma_x(\xi))\,\mathrm{d}\xi\right) - \kappa_2 \exp\left(-\frac{k_x}{\omega}\int_0^x (\mathrm{i}\omega + \sigma_x(\xi))\,\mathrm{d}\xi\right)\right], \\ v^+(x) = \left(-\frac{k_x}{\omega}\frac{\mathrm{i}\omega+\sigma_x}{\mathrm{i}\omega} + \frac{\beta(x)}{\mathrm{i}\omega}\right) \times \left[\kappa_1 \exp\left(\frac{k_x}{\omega}\int_0^x (\mathrm{i}\omega + \sigma_x(\xi))\,\mathrm{d}\xi\right) + \kappa_2 \exp\left(-\frac{k_x}{\omega}\int_0^x (\mathrm{i}\omega + \sigma_x(\xi))\,\mathrm{d}\xi\right)\right]. \end{cases}$$

Imposing continuity of the fields (across the interface $x = 0$), i.e. $p^- = p^+$ and $u^- = u^+$, we obtain $\kappa_1 = 0$ and $\kappa_2 = 1$ (v, T_2 and T_3 are then also continuous). Finally, p is given by

$$p = \mathrm{e}^{-\frac{k_x}{\omega}\int_0^x \sigma_x(\xi)\,\mathrm{d}\xi}\mathrm{e}^{-\mathrm{i}(k_x x + k_y y - \omega t)}. \tag{35}$$

Thus, we have an exponential decay of the wave magnitude.

More generally one can choose $n_{13} = \partial_y\psi,\ n_{23} = \partial_x\psi$ and then adjust ψ to make the model perfectly matched. A more detailed study is in progress. □

Remark. In Lemma 3.1 the condition $A\partial_x N + B\partial_y N = 0$ is not necessary for the well-posdness. Indeed, if N does not satisfy this condition, we will have the zero order term $A(\partial_x N) + B(\partial_y N)$ (assuming σ are $C^1(\mathbb{R})$. One may try to construct a PML relaxing this condition.

4. The convecting case

In this part, we shall consider the two-dimensional compressible Euler equations, linearized around a constant state $(U, V) \neq (0, 0)$; the method described for the quiescent case needs to be modified. In the convecting case, the lemma (9) is no longer true, more precisely there are no invertible operators M and N such that

$$\begin{aligned} MAN - S_x A &= 0, \\ MBN - S_y B &= 0 \end{aligned} \tag{36}$$

to see this, suppose for example $U \neq 0$, A is then invertible and (36) implies

$$S_x MBA^{-1} - S_y BA^{-1} M = 0. \tag{37}$$

First, note that if B is also non-singular, the result yields immediately (taking the determinant of the above expression). If B is singular, let v be an eigenvector of M associated to the eigenvalue λ, (37) leads to

$$MBA^{-1}v = \frac{\lambda S_y}{S_x} BA^{-1}v$$

thus for any positive n, $\lambda(S_y/S_x)^n$ is an eigenvalue of M, which is impossible except if S_x and S_y are fixed equal to the complex roots of unity. In fact, in this case we can take $M = \mathrm{diag}[\lambda, \lambda(S_y/S_x), \lambda(S_y/S_x)^2]$, where (S_y/S_x) is a cubic root of unity. However, this is not possible (σ will depend on ω). Finally, we obtain $\lambda = 0$ and M is not invertible.

To overcome these problems we shall transform the Euler equations in the convective case into a system similar to the aeroacoustic one (for which lemma (9) is true).

For this, we can use the change of variables

$$X(t) = x + Ut \quad \text{and} \quad Y(t) = y + Vt$$

however this transformation leads to a moving PML layer. One can use other changes of variables, for example as in [3] or [2] i.e. (where M is the Mach number)

$$\xi = \sqrt{1 - M^2}x, \quad \eta = y \quad \text{and} \quad \tau = c\sqrt{1 - M^2}t + M\xi. \tag{38}$$

5. Numerical results

To verify the efficiency of our PML models, we present numerical results on a benchmark problem in computational aeroacoustics [13,14]. The initial condition is in the isentropic case an acoustic pulse centered at point x_a,

$$P_0 = \rho_0 = \mathrm{e}^{-(\ln 2)\frac{|x-x_a|^2}{9}}, \quad u_0 = v_0 = 0.$$

The computational domain is $[-60, 60] \times [-60, 60]$, the domain of interest is $[-50, 50] \times [-50, 50]$ surrounded by a layer of thickness $N = 10$. The damping factors $\sigma_i(x_i)$ are chosen (for both simulation) as $\sigma_i(x_i) = \sigma_0(d_i(x_i)/D_i)^3$, where D_i is the thickness of the layer in the x_i direction and $d_i(x_i)$ is the distance from the interface to the point in the layer. According to the results observed in [14], we take $\sigma_0 D/N \cong 8$.

The scheme is a fourth order Runge–Kutta in time, and a seven point finite difference scheme in space.

We present the results for the quiescent medium case. It is shown that the field is well absorbed by the PML layer (the wave arrives at $t = 30$ in the PML) with no noticeable reflection. The Dirichlet condition

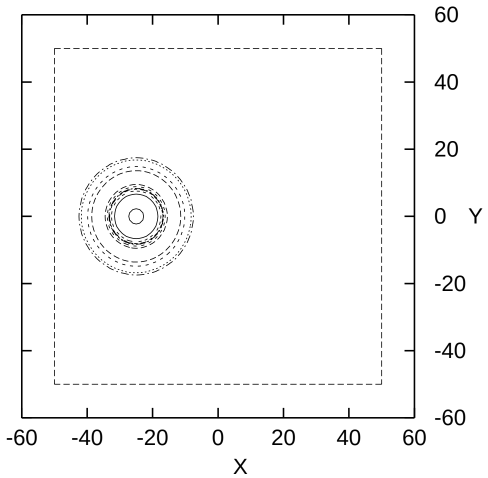

Fig. 1. Pressure contours at $t = 10$.

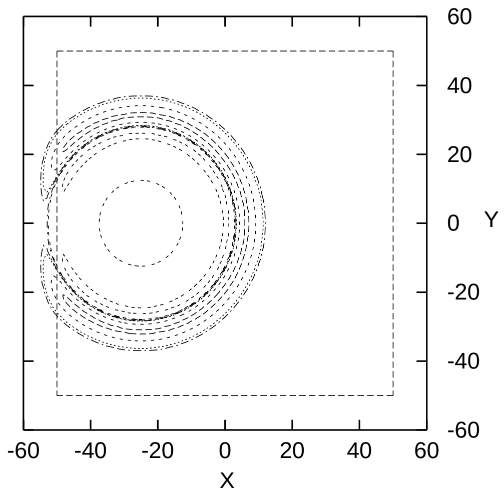

Fig. 2. Pressure contours at $t = 30$.

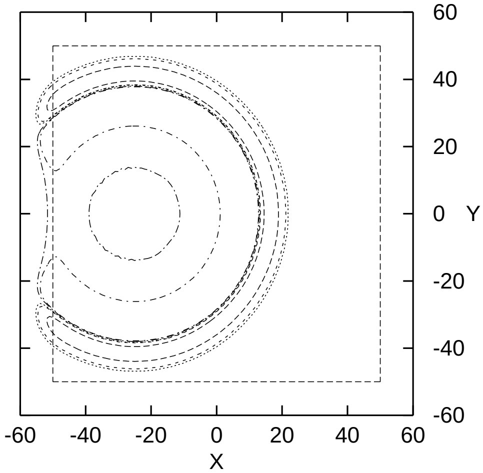

Fig. 3. Pressure contours at $t = 40$.

imposed on the exterior boundary of the PML does not generate spurious reflection and the wave is totally absorbed at $t = 100$.

To measure the reflection due to the PML, the solutions are compared with a reference solution (Sol-Ref) obtained by computing the flow in a much larger domain with the same numerical algorithm (therefore, we compute exactly the "effect" of the PML).

We shall also plot the rate of absorption, τ, given by

$$\tau = \frac{|P_{\text{Sol-Ref}} - P_{pml}|}{|P_{\text{Sol-Ref}}|} \times 100. \tag{39}$$

In Figs. 1 and 2 we plot the pressure contours of the solution, respectively, at $t = 10$ and $t = 30$; time $t = 30$ is interesting as the wave arrives to the left PML layer with no spurious reflection (see Figs. 3 and 4).

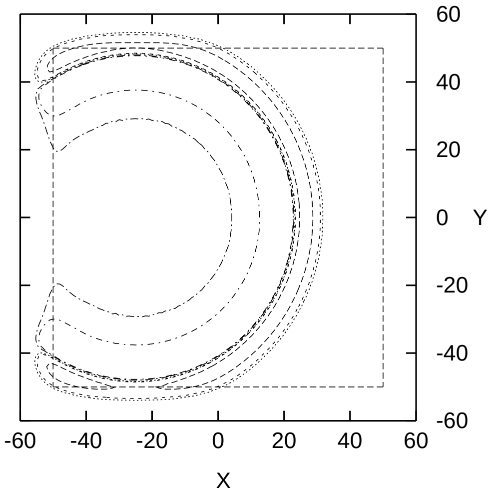

Fig. 4. Pressure contours at $t = 50$.

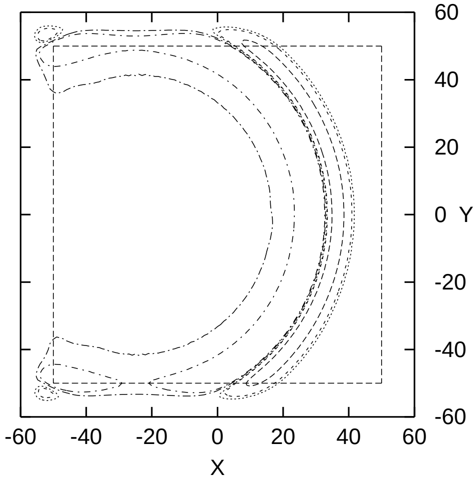

Fig. 5. Pressure contours at $t = 60$.

The wave progresses without reflection and has not yet reached the external boundary. In Figs. 5 and 6 the wave reaches the external boundary (where a Dirichlet boundary condition is imposed); as can be seen the corner does not generates problems. These two snapshots of the pressure show how well the outgoing waves are absorbed (see Figs. 7 and 8), we can note that the PML layer affects a small region near the interface (this is due to the numerical scheme, described in [27]).

The model given by (28) gives similar results (corresponding to the simplest model $\alpha = 0, \beta = 1$). We can note that the model is less absorbing than the classical one. Moreover, we observe a small discretization error (Fig. 9) due to choice of β.

The wave progresses without reflection and has not yet reached the external boundary.

In Figs. 5 and 6 the wave reaches the external boundary (where a Dirichlet boundary condition is imposed); as can be seen the corner does not generates problems (see Figs. 10–12).

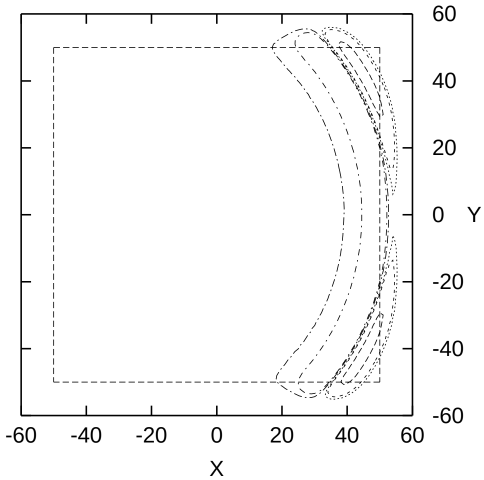

Fig. 6. Pressure contours at $t = 80$.

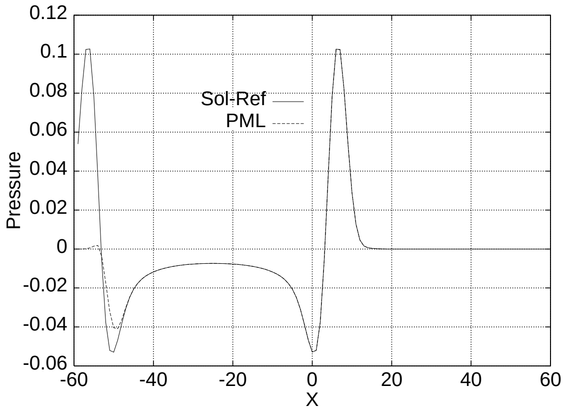

Fig. 7. Pressure value along $y = 0$ at $t = 30$.

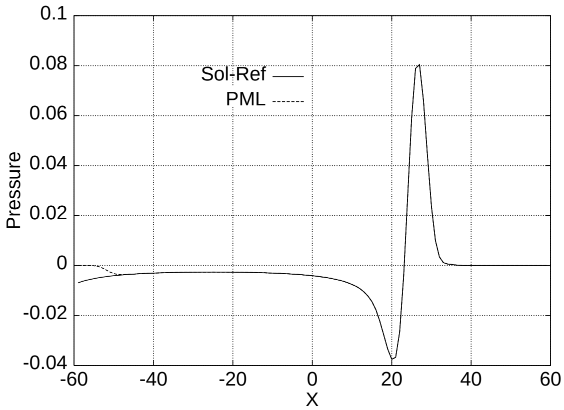

Fig. 8. Pressure value along $y = 0$ at $t = 50$.

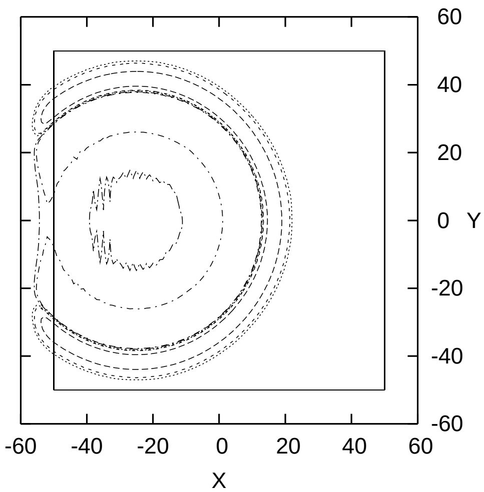

Fig. 9. Pressure contours at $t = 40$.

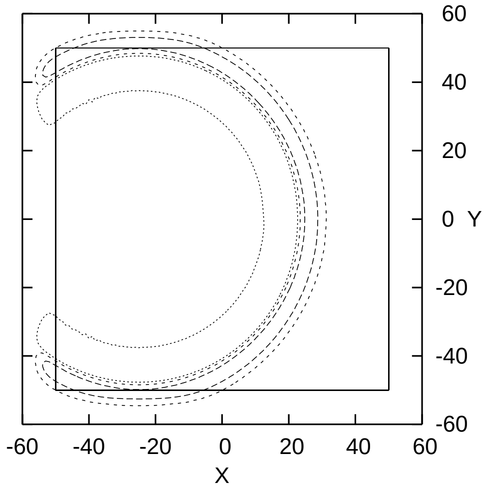

Fig. 10. Pressure contours at $t = 50$.

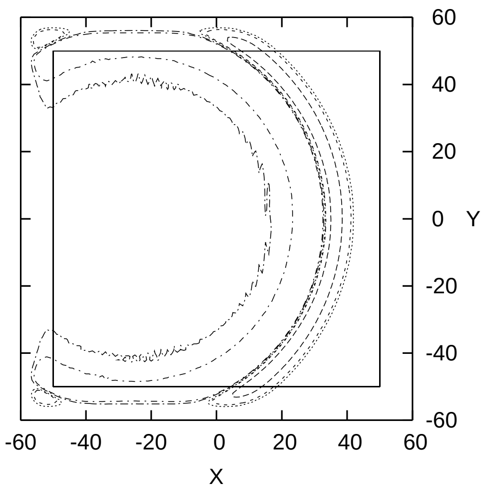

Fig. 11. Pressure contours at $t = 60$.

6. Conclusion

The technique proposed in this section, to obtain a well-posed PML model for Euler equations, relies on an algebraic lemma leading to a strongly hyperbolic system.

The model obtained is identical to the model obtained in [9,25] however the derivation presented here can be extended to various hyperbolic systems.

This method preserves all the advantages of the Bérenger model while retaining symmetry. Moreover, this model uses primitive variables unlike the Bérenger one, thus it is effectively easier to integrate into an existing code.

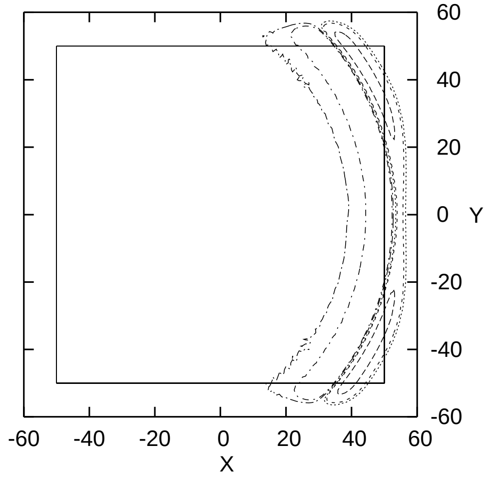

Fig. 12. Pressure contours at $t = 80$.

The development of a PML model for a non-constant mean flow remains a significant challenge and is the subject of current research.

Acknowledgements

The author expresses his gratitude to Professor Laurence Halpern, University Paris 13, for inspiring and enlightening conversations.

References

[1] S. Abarbanel, D. Gottlieb. On the construction and analysis of absorbing layers in CEM, in: ACES 13'th Annual Review of Progress in Applied Computational Electromagnetics, 1997, pp. 876–883.
[2] S. Abarbanel, D. Gottlieb, S. Hesthaven, Well-posed perfectly matched layers for advective acoustics, Journal of Computational Physics 154 (1999) 266–283.
[3] A. Bayliss, E. Turkel, Far field boundary conditions for compressible flows, Journal of Computational Physics (1982) 182–199.
[4] J.P. Bérenger, Three-dimensional perfectly matched layer for the absorption of electromagnetic waves, Journal of Computational Physics 114 (1994) 185–200.
[5] B. Yang, P. Petropoulos, Plane-wave analysis and comparison of split-flied, biaxial, and uniaxial pml methods as abcs for pseudospectral electromagnetic wave simulations in curvilinear coordinates, Journal of Computational Physics 146 (1998) 747–774.
[6] W. Chew, W. Weedon, A 3d perfectly matched medium from modified Maxwell's equations with stretched coordinates, Microwave and Optical Letters (1994) 599–604.
[7] F. Collino, P. Monk, Conditions et couches absorbantes pour Maxwell, Technical Report 18, INRIA, aspects récents en méthodes numériques pour les équations de Maxwell, 1998.
[8] F. Collino, C. Tsogka, Application of the pml absorbing layer model to the linear elastodynamic problem in anisotropic heterogenous media, Technical Report 3471, INRIA, 1998.
[9] S.D. Gedney, An anisotropic perfectly matched layer-absorbing medium for the truncation of fdtd lattices, IEEE Transactions on Antennas and Propagation 44 (1996) 1630–1639.
[10] D. Givoli, Non-reflecting boundary conditions, Journal of Computational Physics 94 (1991) 1–29.
[11] L. Halpern, Artificial boundary conditions for incompletly parabolic perturbation of hyperbolic systems, SIAM (1991) 1256–1283.
[12] J.S. Hesthaven, The analysis and construction of perfectly matched layers for the linearized Euler equations, Technical Report 97-49, ICASE, September, 1997.

[13] J.S. Hesthaven, On the analysis and construction of perfectly matched layers for the linearized Euler equations, Journal of Computational Physics 142 (1) (1998) 129–147.
[14] F.Q. Hu, On absorbing boundary conditions for linearized Euler equations by a perfectly matched layer, Journal of Computational Physics 129 (1996) 201–219.
[15] M. Israeli, S.A. Orszag, Approximation of radiation boundary conditions, Journal of Computational Physics 41 (1981) 115–135.
[16] H.-O. Kreiss, J. Lorenz, Initial-Boundary Value Problems and the Navier–Stokes Equations, Academic Press, New York, 1989.
[17] P.A. Mazet, S. Paintandre, A. Rahmouni, Interprétation dispersive du milieu PML de Bérenger, Comptes Rendus de l'Academie des Sciences 327 (1998) 59–64.
[18] P. Petropoulos, Reflectionless sponge layers as absorbing boundary conditions for the numerical solution of maxwell equations in rectangular, cylindrical, and spherical coordinates, SIAM Journal of Applied Mathematics 60 (3) (2000) 1037–1058.
[19] A. Rahmouni, A mathematical analysis of the perfectly matched layer method for electromagnetism, in: Mathematical and Numerical Aspects of Wave Propagation, SIAM, Philadelphia, PA, 1998.
[20] A. Rahmouni, Un modèle PML bien posé pour les équations d'Euler linéarisées, Comptes Rendus de l'Academie des Sciences 331 (2000) 159–164.
[21] A. Rahmouni, Well posed PML models for various hyperbolic systems, Ph.D. Thesis, Université Paris 13, 2000.
[22] A. Rahmouni, A well posed PML model for elastodynamic, in: Mathematical and Numerical Aspects of Wave Propagation, SIAM, Philadelphia, PA, 2000.
[23] C.M. Rappaport, Interpreting and improving the pml absorbing boundary condition using anisotropic lossy mapping of space, IEEE Microwave Guided Wave Letters (5) (1995) 90–92.
[24] J.A. Roden, S.D. Gedney, Convolutional pml (cpml): an efficient fdtd implementation of the cfs-pml for arbitrary media, Microwave and Optical Technology Letters 27 (2000) 334–339.
[25] Z.S. Sacks, D.M. Kingsland, R. Lee, J.F. Lee, A perfectly matched anisotropic absorber for use as an absorbing boundary condition, IEEE Transactions on Antennas and Propagation 43 (1995) 1460–1463.
[26] A. Taflove (Ed.), Advances in Computational Electrodynamics: The Finite-Difference Time-Domain Method, Artech House, Boston, MA, 1998.
[27] C.K.W. Tam, J.C. Webb, Dispersion-relation-preserving finite difference schemes for computational acoustics, Journal of Computational Physics 107 (1993) 262–281.
[28] L. Tourette, Artificial boundary conditions for the linearized compressible Navier–Stokes equations, Journal of Computational Physics (137) (1997) 1–37.